



## Parylene-based integrated wireless single-channel neurostimulator

Wen Li<sup>a,\*</sup>, Damien C. Rodger<sup>b</sup>, Anderson Pinto<sup>b</sup>, Ellis Meng<sup>c</sup>, James D. Weiland<sup>b</sup>, Mark S. Humayun<sup>b</sup>, Yu-Chong Tai<sup>a</sup>

<sup>a</sup> Department of Electrical Engineering, California Institute of Technology, Pasadena, CA 91125, USA

<sup>b</sup> Keck School of Medicine, University of Southern California, Los Angeles, CA 90033, USA

<sup>c</sup> Department of Biomedical Engineering, University Park Campus, University of Southern California, Los Angeles, CA 90089, USA

### ARTICLE INFO

#### Article history:

Received 15 April 2009

Received in revised form

28 November 2009

Accepted 4 March 2010

Available online 16 March 2010

#### Keywords:

BIONs

Implantable MEMS

Integrated neurostimulator

Parylene C

Retinal prosthesis

Wireless

### ABSTRACT

This paper presents the design, fabrication, and functional testing of a fully implantable, flexible, Parylene-enabled neurostimulator that features single-channel wireless stimulation capability [1]. This system comprises a fold-and-bond microelectromechanical systems (MEMS) coil for wireless power and data transmission, a BION 1-3 CMOS stimulator chip, discrete capacitors, as well as a carrier substrate with two platinum stimulating electrodes and interconnections for system assembly. The physical geometries of the devices are designed for use in retinal implantation with the specifications determined from the implantation results in canine eyes. The coil and carrier substrate are separately fabricated using a Parylene-metal skin technology. The unique properties of Parylene C allow these MEMS devices to be flexible and biocompatible, facilitating surgical procedure. The system assembly is achieved by interconnecting individual components together on the carrier substrate with a biocompatible silver epoxy. A 10  $\mu\text{m}$  layer of Parylene C is selectively deposited on the integrated system to protect it from corrosive eye environment. The system functionality is verified using a telemetry link setup, and single-phase pulses with amplitudes ranging from 7 to 8.5 V are detected.

© 2010 Elsevier B.V. All rights reserved.

### 1. Introduction

Nervous system damages (e.g. brain trauma, spinal cord injury, and retinal diseases) result in permanent physical disabilities to millions of people worldwide [2,3] and are presently incurable conditions. Potential treatments such as neural transplantation and stem cell therapy [4–6] are promising but their implementation faces great challenges due to the lack of clinical practice protocols, high costs, and political issues. Artificial neural prostheses, which utilize electronic devices as interfaces to central and peripheral neural systems, have been increasingly accepted to partially treat neurological disorders and diseases. Many different approaches have been investigated, using electrical signal to stimulate neurons and muscles for controlling of limbs and organs, or to elicit sensory sensation for feeling, hearing, or seeing. Numerous applications include limb prostheses for spinal cord injury and stroke, sacral nerve stimulations for bladder emptying, deep brain stimulation (DBS) for essential tremor and the tremor of Parkinson's disease, cochlear prostheses for restoring hearing, and retinal prostheses

for outer retinal degenerative diseases such as age-related macular degeneration (AMD) and retinitis pigmentosa (RP), to name just a few [7–11].

In recent decades, integrated wireless microsystems emerge and provide breakthrough opportunities for implantable neural prosthesis. Microfabrication technologies can effectively increase the degree of miniaturization and system complexity. Wireless power and data signal transmission through electromagnetic fields avoids batteries or permanent wired connections, and thus reduces surgical complexity as well as undesired physical damages to patients. Among the aforementioned examples of neural prostheses, an epiretinal prosthesis is one of the most prominent prosthetic interfaces that will benefit from wireless microsystem technologies. An epiretinal implant system typically comprises (1) radio-frequency (RF) coils for transferring power and data between intraocular units and external data acquisition units, (2) integrated circuitry for converting signal and providing stimulus to retina, and (3) a multielectrode array for stimulating neural cells on the inner retina (Fig. 1). For applications that involve completely intraocular implantation in human eyes, the following requirements on the system and encapsulation method are critical: (1) sufficiently high spatial selectivity, (2) biocompatibility and low cytotoxicity, (3) enough flexibility to conform to anatomical curvatures of eyeballs, minimize tissue damage, and facilitate surgical procedure. Current technologies using flexible polymer-based microsystems

\* Corresponding author at: Michigan State University, Electrical & Computer Engineering, 2120 Engineering Building, East Lansing, MI 48824, USA.

Tel.: +1 517 353 7832; fax: +1 517 353 1980.

E-mail address: [wenli@egr.msu.edu](mailto:wenli@egr.msu.edu) (W. Li).

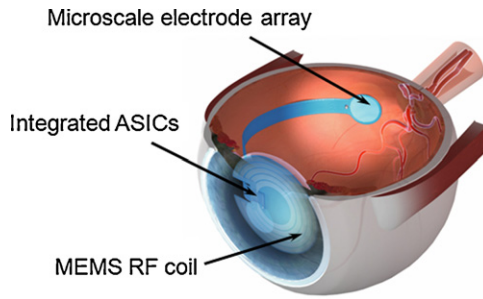


**Fig. 1.** Conceptual schematic of an epiretinal prosthesis showing main components and their placement.

for epiretinal implants are still in developmental stage [12–14] and few have actually been transferred to the clinical practice due to challenges with respect to material selection, device miniaturization, as well as fabrication and integration methods.

Our goal is to address these existing issues, by integrating Parylene-based microelectromechanical systems (MEMS) devices (microcoils and electrode arrays) with other discrete components (application specific integrated circuits (ASICs), capacitors, etc.) to develop flexible and biocompatible wireless neural implants. In this work, we present the first completely Parylene-based functional neural stimulator, which consists of a MEMS coil and an electrode array integrated with a single-channel stimulator chip. For the first prototype, MEMS devices are made separately, and assembled with other system components using biocompatible silver epoxy. A Parylene–metal skin technology has been developed, which allows us to microfabricate RF coils and high-density multi-electrode arrays in a process compatible way [15,16]. Parylene C is chosen as the main substrate and packaging material because of its favorable properties, such as flexibility (Young's modulus  $\sim 4$  GPa), optical transparency, chemical inertness, and biocompatibility [17]. In fact, Parylene C is an ISO 10993 and United States Pharmacopeia (USP) Class VI biocompatible material, the highest biocompatibility and implant clearance among plastics. Upon intraocular implantation in two rabbits for 6 months, Parylene C is shown to generate no detectable immune response affecting their retinas [18]. These

results indicate that Parylene C is a biocompatible material suitable for long-term intraocular retinal prostheses.

## 2. System design

**Fig. 2** depicts the system schematic of the single-channel simulator, which consists of a complementary metal–oxide–semiconductor (CMOS) chip, two capacitors, a specially designed RF MEMS coil, and a carrier substrate. The chip is a single-channel stimulator which was initially developed by Loeb and co-worker to mimic muscle spindle function for patients with muscle paralysis [8]. When implanted into paralyzed muscles, power and command signals can be delivered to the chip through inductive coupling over a 480–500 kHz power carrier generated in an external personal trainer. Then the chip can emit precisely timed stimulation pulses with a highly regulated amplitude and pulse-width. **Fig. 3** shows a BION 1–3 chips used in our experiments, and the pad functionalities are described in the right hand table. This chip has physical dimensions of  $\sim 1$  mm in width,  $\sim 2.33$  mm in length, and  $\sim 257 \mu\text{m}$  in thickness. There are five pads on the BION chip approximately  $120 \mu\text{m}$  by  $74 \mu\text{m}$  in size, and the distance between adjacent pads is about  $110 \mu\text{m}$ .

A dual-metal-layer coil is designed as the main component for wireless power and data transmission. The self-inductance of such a MEMS coil is limited by its small dimensions, and can be calculated using the following equation [19]:

$$L_s = 2\pi d N^2 \times 10^{-9} \left[ \left( \ln \frac{4d}{t} \right) \left( 1 + \frac{t^2}{24d^2} \dots \right) - \frac{1}{2} + \frac{43t^2}{288d^2} \dots \right] \text{ (Henry)}, \quad (1)$$

where  $N$  is the total number of turns,  $d$  (in cm) is the mean diameter of the coil, and  $t$  (in cm) is the coil width. Two ceramic chip capacitors (AVX Corporation, Myrtle Beach, SC, USA) are also incorporated into the system for circuit function, as shown in **Fig. 2**.  $C_1$  is a frequency tuning capacitor in parallel with the receiving coil to achieve a resonant frequency of  $\sim 500$  kHz, and  $C_2$  is a charge storage capacitor which has a capacitance of  $\sim 22$  nF. The size of these capacitors is approximately 1 mm in length, 0.5 mm in width, and 0.56 mm in thickness. Finally, the carrier substrate is designed for system assembly, which comprises a flexible cable, interconnection leads and contact pads, and two stimulus electrodes of which one serves as the signal terminal and the other as the floating ground.

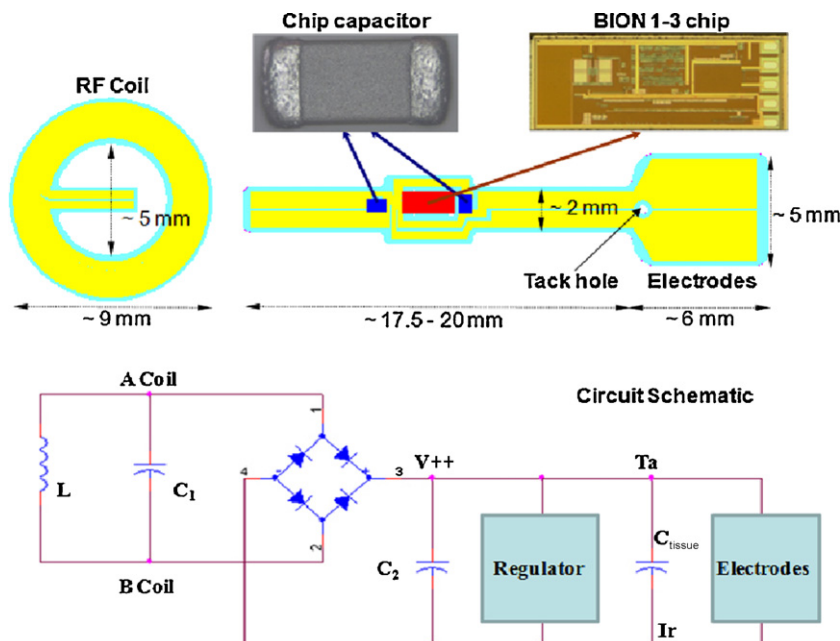


**Fig. 2.** System schematic of the single-channel stimulator and the corresponding circuit layout, showing the connections between individual components.

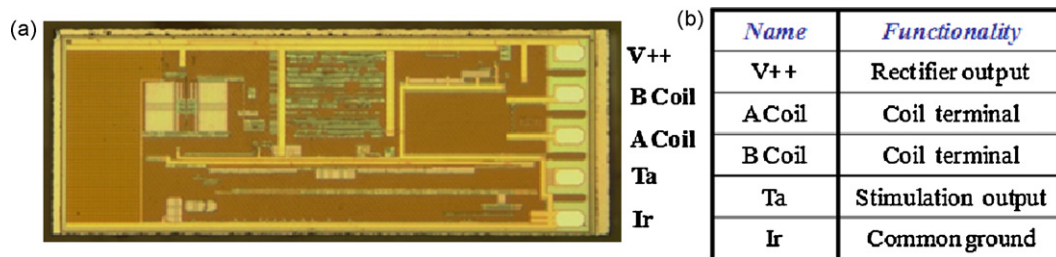


Fig. 3. (a) Microscope image of a BION 1-3 chip. (b) Pad function of the chip.

Overall physical dimensions of the MEMS coil and the carrier substrate need to meet specifications used in retinal implantation. Due to the small volume and complex anatomy of eyes, it is necessary to evaluate possible geometries in eyes prior to finalizing the designs of the devices. It is also important to verify the robustness of the devices and materials under surgical manipulation. Thus, mechanical models with various dimensions are first fabricated and implanted in canine eyes to study the system geometrical feasibility inside the eye, as shown in Fig. 4. In this experiment, carrier substrates are made of Parylene C thin films (PDS 2120 system, Special Coating Systems, Indianapolis, IN, USA) using a photoresist mask and oxygen plasma etching in a reactive ion etching (RIE) system (Semi Group Inc. T1000 TP/CC). Plastic dummy coils and chips are then glued onto the carrier substrates using biocompatible epoxy EPO-TEK 301-2 (Epoxy Technology, Billerica, MA, USA), simulating the system integration of various key components. The animal surgery is operated at the Keck School of Medicine of the University of Southern California. During the implantation, the coil site is placed right beneath the cornea, in the anterior chamber of canine eyes, less than 1 mm from external air. After lens extraction, the flexible cable is passed through the anterior and posterior lens capsule into the vitreous cavity, leaving the chip site floating in the vitreous cavity. Vitrectomy is then performed and the electrode array site is attached on top of the inner retina using a retinal tack modified by the addition of a PDMS washer. Based on preliminary surgical results, optimal device dimensions for canine eyes are determined as indicated in Fig. 2. Devices for human implantations can be simply modified by reducing the cable length in order to accommodate the smaller space of the vitreous cavity in human eyes.

### 3. Fabrication

In order to reduce fabrication complexity, the coil and the carrier substrate are fabricated and calibrated respectively. Then the system is assembled by interconnecting individual components on the carrier substrate with a conductive silver paste. Detailed fab-

rication is divided into three steps and described in the following sections.

#### 3.1. Carrier substrate fabrication

To build the flexible substrate, a 200 nm layer of metal is e-beam (SE600 RAP, CHA Industries, Fremont, CA, USA) evaporated on a Parylene C coated silicon substrate. Then the metal is patterned using a lift-off method to form connection pads, interconnection leads, and electrode array [16]. Platinum is selected as the primary electrode material due to its optimal stimulation capability and biocompatibility. Parylene C-based arrays of thin-film platinum electrodes have shown excellent biostability when chronically implanted in contact with canine retinas for 6 months [16]. Furthermore, platinum and Parylene are known to have good adhesion, requiring no additional adhesion metal layer during fabrication. After metal patterning, another layer of Parylene C is deposited to seal the entire structure, followed by oxygen plasma etching with a photoresist mask to define the contour of the carrier substrate, as well as to open the electrode sites and the contact vias. Finally, the device is peeled off from the silicon substrate in a water bath and dried in air. Fig. 5 illustrates the detailed process for making the carrier substrate, where steps (b)–(d) describe the lift-off technology for platinum patterning.

Fig. 6 presents a fabricated carrier substrate. This device has a total thickness of approximately 10  $\mu\text{m}$ . Three extra pads are added on the chip site for testing purpose and can be removed after system integration. The microscope image in Fig. 6 shows a special chip site design where Parylene ribbons are etched in a way such that the chip can be held in place and self-aligned to the contact vias on the substrate during system assembly. The array site contains a 450  $\mu\text{m}$  diameter tack hole so that it can be attached to the retina with the retinal tack during implantation.

#### 3.2. RF MEMS coil fabrication

A fold-and-bond technology is involved in the MEMS coil fabrication [20]. First, a planar Parylene–metal–Parylene sandwich structure is built with two coils arranged in series (Fig. 8). The fabrication process is shown in Fig. 7. Briefly, a 3  $\mu\text{m}$  layer of gold is deposited on a Parylene coated substrate and patterned with metal etching process. Then Parylene deposition is performed on top of metal, followed by oxygen plasma etching to open contact vias. Photoresist serves as a sacrificial layer so the structures can be released from the substrate by dissolving photoresist in acetone.

After the planar structure is microfabricated, it is folded into two layers and stacked together with the assistance of two glass slides. Aluminum sheets are inserted between the Parylene surface and the glass slides to prevent Parylene from sticking to glass. External pressure is applied by stacking a  $\sim 2$  lbs metal plate on top of a 75 mm  $\times$  50 mm glass slide, allowing Parylene-to-Parylene bonding at modest temperatures. After that, the whole unit is placed in a vacuum oven (T-M Vacuum Products, Inc., Cinnamin-

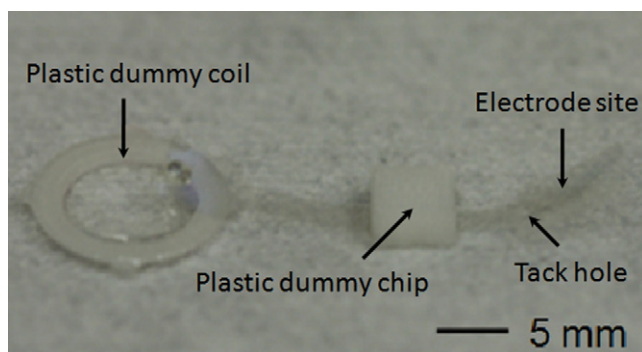


Fig. 4. A dummy structure for canine implantation.

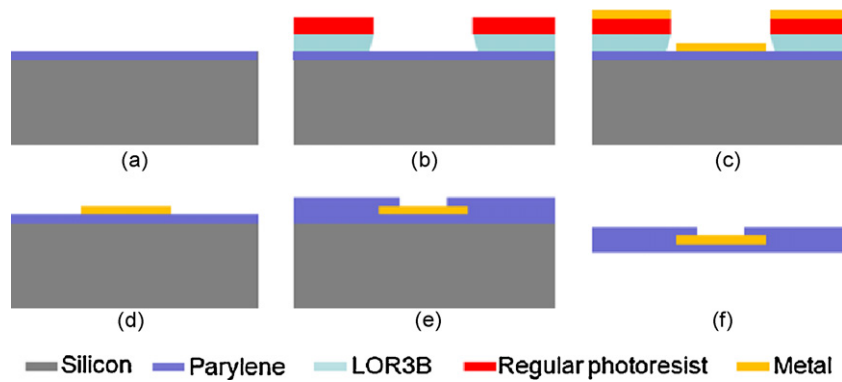


Fig. 5. Fabrication process of the Parylene-based carrier substrate.

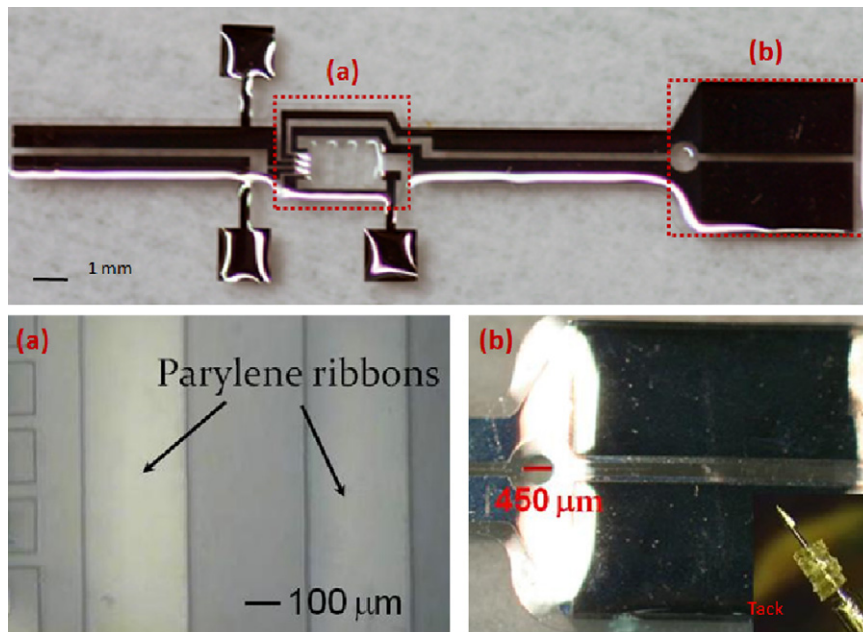


Fig. 6. A fabricated carrier substrate with electrodes, interconnection leads and contacts. (a) Parylene ribbons for holding the BION chip. (b) A 2-electrode array with a tack hole.

son, NJ, USA) with the chamber pressure of  $\sim 10$  Torr for bonding. The oven temperature ramps from room temperature to bonding temperature, and then soaks at the bonding temperature for 2 days, followed by slowly cooling to the room temperature. Nitrogen backfill is introduced to the chamber in order to equalize the chamber temperature. Experiments are performed at a setting temperature range of  $180$ – $250^\circ\text{C}$ , and bonding results are evaluated by visual inspection. The results demonstrate that the vacuum pressure of 10 Torr can prevent Parylene from undesired oxidation at elevated temperatures so that the device can remain flexible after bonding. It is also found that good Parylene-to-Parylene bonding occurs in samples annealed at temperatures higher than  $230^\circ\text{C}$ . It should be noted that the bonding temperature has to be lower than the melting temperature of Parylene C

( $290^\circ\text{C}$ ), as strong recrystallization can happen beyond this point [21].

A fabricated coil is shown in Fig. 8, comprising two layers of metal with 10 turns in each layer. In-and-out leads are connected to the carrier substrate from the center to facilitate the surgical procedure. Through vias are designed to overlap with the contact pads so that the interconnections to the carrier substrate can be formed from either side. The electrical properties of this coil are measured with an Agilent 34401A multimeter and the HP 4192A LF impedance analyzer (HP/Agilent Technologies Inc., Santa Clara, CA, USA), showing an inductance of approximately  $2.24\ \mu\text{H}$  and a DC resistance of approximately  $15.82\ \Omega$ . A  $Q$  factor of 0.45 is calculated at the operation frequency of 500 kHz. Theoretically, thicker metal can lower the intrinsic resistance of the coil to achieve higher  $Q$

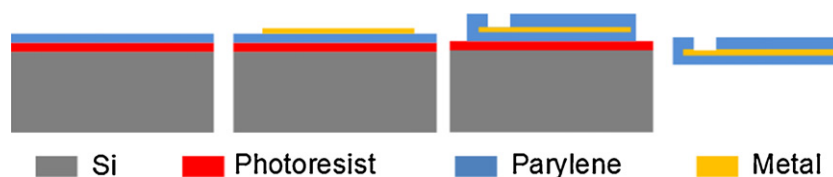
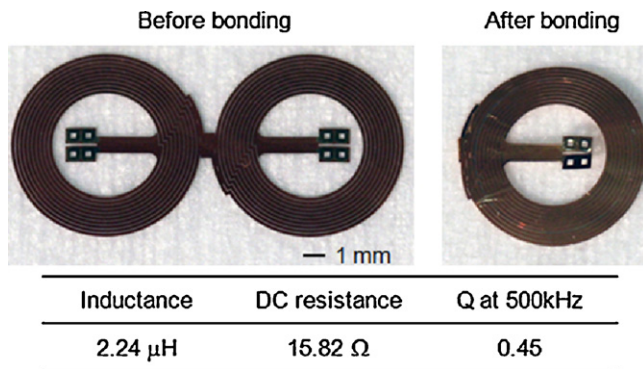


Fig. 7. Fabrication process of Parylene-metal-Parylene sandwich structure.





**Fig. 8.** A fabricated fold-and-bond coil with two layers of metal. The electrical characteristics are measured and given in the table.

factor and better performance, but e-beam evaporated metals are often limited in film thickness due to process cost.

### 3.3. System assembly and packaging

For hybrid system assembly, discrete components (the BION chip, the coil and the capacitors) are aligned to corresponding interconnection vias on the carrier substrate. A small amount of biocompatible silver epoxy EPO-TEK H20E is then applied on the

contacts and cured at 80 °C for 3 h in a convection oven. The conductive epoxy serves two purposes: to form the interconnections between the components as well as to bond the components onto the substrate. Fig. 9 shows an assembled single-channel stimulator system, and close-up views of the interconnections for each component.

Because the BION chip used in our experiment has only five pads, hand assembly can be used as a temporary solution for fast integration. However, a major problem of manual assembly is the inability to control epoxy dosage when applied by hand. Short circuits can be created if too much epoxy is applied, and epoxy reflow can also happen during high temperature curing, resulting in short circuits between adjacent pads. For circuitry with high-density pad layouts, this hand assembly is no longer feasible, and thus a wafer level integration technology becomes necessary [22].

Another big concern is the isolation of the silver epoxy from the eye environment. Human eye is known as a delicate and sensitive organ. Any toxin released from the epoxy can cause inflammation and infection. In addition, eye fluids are corrosive to exposed metals [23], which can reduce the durability of silver epoxy bonding, and finally result in open circuits. To overcome these challenges,  $\sim 10 \mu\text{m}$  Parylene C is coated over the entire system just leaving the electrode sites open to protect the circuitry from corrosive eye fluids. The packaging performance of Parylene C has been studied using accelerated-lifetime soak tests in related work [24]. Preliminary results indicate that Parylene C protected metal can remain

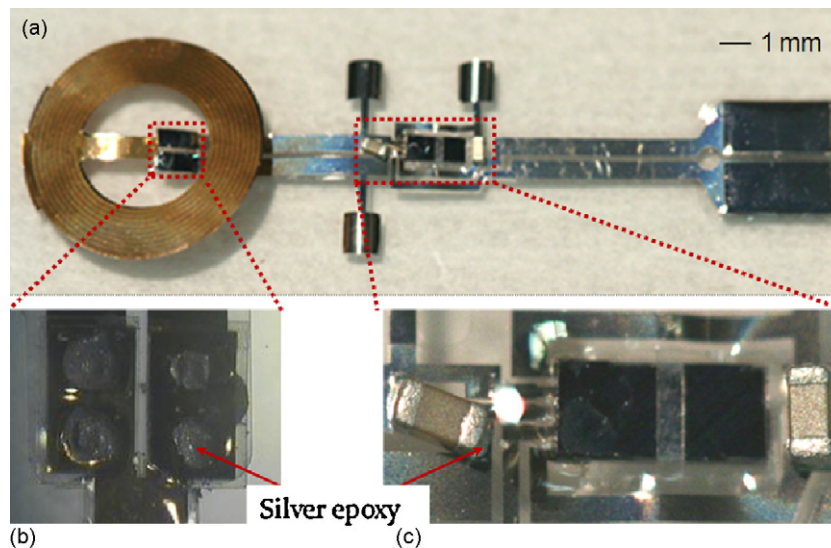


**Fig. 9.** (a) An assembled BION system. (b) Interconnects of coil contacts formed with biocompatible conductive silver epoxy. (c) Interconnects of chip and capacitor contacts formed with biocompatible conductive silver epoxy.

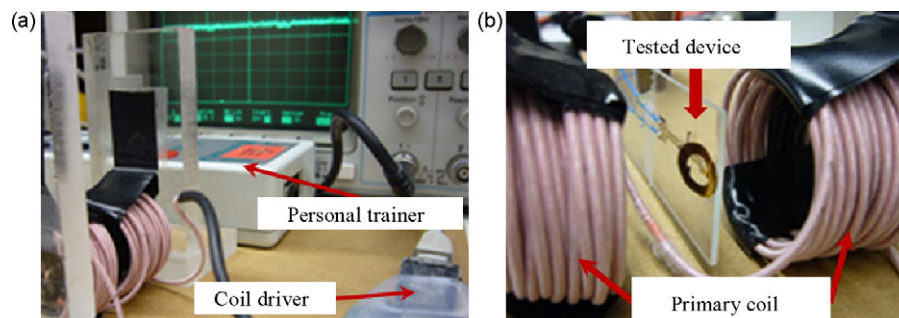


**Fig. 10.** (a) A telemetry setup for functionality test of the assembled BION system. (b) A close-up image showing the tested system placed between the primary coil.

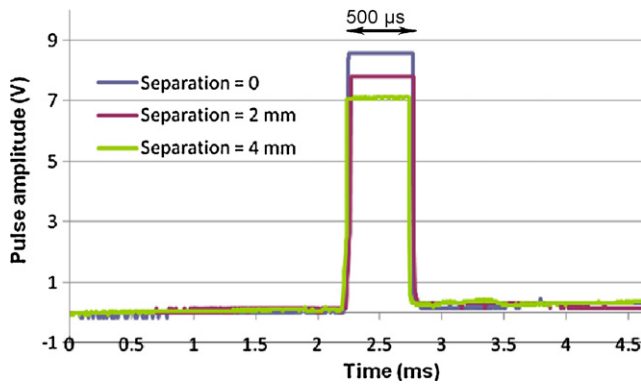


Fig. 11. Recorded stimulation pulses at different separation distances between two coils.

intact in saline (0.9% NaCl) at body temperature (37 °C) for over 20 years, which is very promising for our application.

#### 4. Test results and discussions

The system functionality is verified using a telemetry link setup (Fig. 10). The primary stage, which comprises a personal trainer unit, a class-E coil driver, and a hand-wound transmitting coil, can generate a power carrier of approximately 500 kHz. The personal trainer stores command programs personalized for individual subjects, records the time and duration of treatment, and transfers this information to an external computer for real time monitoring. Upto three programs can be preloaded into the memory of the personal trainer [25]. The coil driver is connected to the personal trainer through a custom made adapter. The transmitting coil has an inductance of  $\sim 46.4 \mu\text{H}$  and a  $Q$  factor of  $\sim 118$  at 500 kHz. Litz wires 1025–44 SPN are used for winding the primary coil in order to reduce the skin effect and proximity effect losses. The transmitting coil is built in a solenoid shape to establish a more uniform electromagnetic field inside the coil. It is also known that the induced voltage at the receiving coil increases proportionally with the increase of magnetic flux going through the inductive link. Therefore, ferrite cores are incorporated in the transmitting coil to magnify electromagnetic field and improve voltage transfer efficiency.

*In vitro* measurements have been conducted in air using this setup, and output signals of the integrated stimulator are monitored by connecting two electrodes directly to an HP 54645A oscilloscope. The distance between the two coils is varied during testing, and a maximum detectable range of  $\sim 4$  mm is found. The operation range is relatively short, suffering from the low  $Q$  factor of the receiving coil as expected. The recorded stimulating pulses at the different separation distances are given in Fig. 11, showing a pulse width of approximately 500  $\mu\text{s}$ , and amplitudes varying from 7 to 8.5 V.

In order to estimate the power transfer capability of the MEMS coil, voltage across the receiving coil terminals and current delivered to the chip are measured. Fig. 12 shows typical waveforms of the transferred voltage and current, indicating a resonant frequency of  $\sim 505$  kHz and a  $\sim 25^\circ$  phase drift between voltage and current. As mentioned earlier, the tuning capacitor is a commercially available chip capacitor, which has limited options for capacitance values. Therefore, it is difficult to fine tune the resonant circuit to achieve precise synchronization. Delivered power at different separation distances is also investigated, as shown in Fig. 13. It can be seen that our MEMS coil can transfer a maximum power of  $\sim 43$  mW through this inductive link at a separation distance of 1 mm. As the separation distance increases to 2 mm, the power drops dramati-

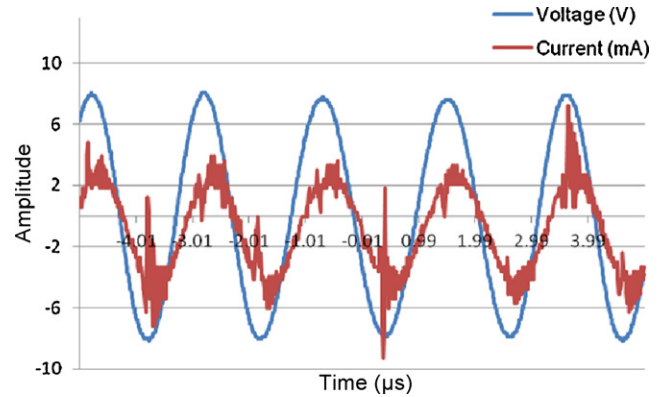


Fig. 12. Typical waveforms of transferred voltage and current to the chip.

cally by 62%, mainly due to the divergence of electromagnetic field. When delivered power is less than 10 mW, no stimulating pulse can be detected from the output.

Similar power transfer measurements have also been performed by immersing the integrated stimulator in regular saline solution to simulate *in vivo* conditions. Preliminary experimental results have shown that the maximum detectable range of this telemetry link is decreased to approximately 2 mm. This significant reduction ( $\sim 50\%$ ) is attributed to a substantial environmental permittivity change in the liquid medium as compared with air, which results in the increase of magnetic energy losses into the saline and a low  $Q$  factor of the MEMS coil [26].

Typical detection distance for retinal prostheses in current clinical applications is estimated to be approximately 15 mm, which is defined as the coaxial separation distance between the implanted coil and the external coil. In our system, the internal coil is placed right beneath the cornea, and the limiting factor in reducing this distance is the large separation of external coil from eye surface for safety reason. To accommodate such requirements and increase the practicality of our stimulator, further improvement can be made to increase the detectable range by optimizing coil design, such as increasing metal thickness and/or the number of metal layers, to enhance the coil  $Q$  factor and the power transfer efficiency. Particularly, for a fold-and-bond coil used in this integrated system, the coil  $Q$  factor is proportional to the number of folds and can be enhanced by  $n$ -times when  $n$  single layers of Parylene–metal thin films are stacked and bonded together [20].

The functionality of the integrated system has been successfully demonstrated in both air and saline. Some efforts have been carried out to test the mechanical reliability of the integrated system in rabbit eyes, as well as to optimize the surgical procedure. Fig. 14 shows an example of the acute implantation, in which an integrated system is implanted in a rabbit eye. After implantation, the

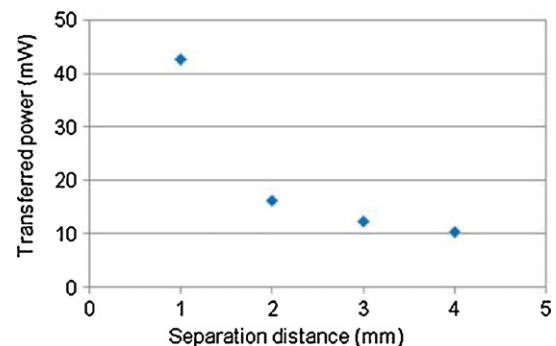
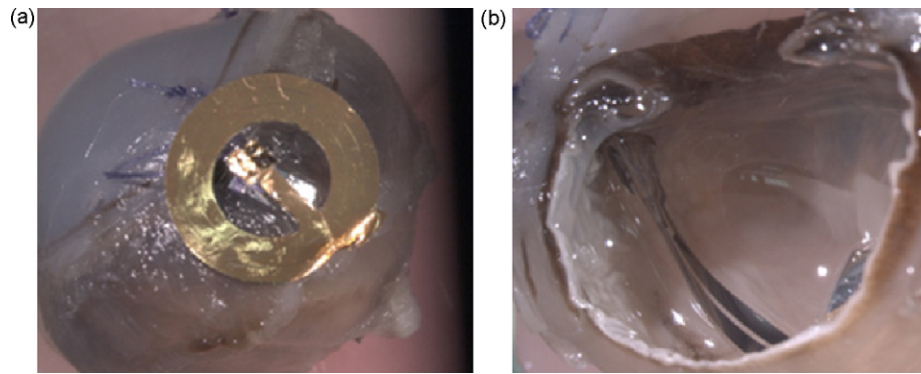


Fig. 13. Transferred power at different separation distances between two coils.



**Fig. 14.** Acute implantation images of an integrated system in a rabbit eye, showing: (a) the coil sitting in front of the iris; (b) the flexible cable and array implanted in the vitreous cavity.

subject is sacrificed and its eyeball is soaked in forming solution for 1–2 weeks to maintain the eyeball shape. Then the eyeball is removed from the solution and cut into halves in order to examine the implanted device. Preliminary outcomes suggest the implanted device can mechanically withstand the surgical procedure fine. Future work will aim to improve the power transfer performance of the telemetry link as well as to verify the system functionality and biostability using *ex-vivo* testing and *in vivo* implants in rabbit subjects.

## 5. Conclusion

A Parylene-based single-channel neural stimulator has been designed, and the first prototype has been successfully microfabricated and assembled. *In vitro* active measurements are performed to verify the functionality of the integrated system. The test results demonstrate that the BION chip can be driven by the MEMS coil within a 4mm separation distance in air. Output pulses with  $\sim 500 \mu\text{s}$  pulse width and greater than 7 V amplitude are detected from the stimulating electrode. Preliminary animal implantation result indicates that the integrated system is mechanically reliable and surgically compatible. We are expecting to implant the device in animal subjects to further characterize its system performance *in vivo*. Although specifically tailored to the needs of retinal prostheses, this system integrates Parylene-based MEMS devices with discrete electrical components and ASICs, and thus enables a new range of true system solutions for both biomedical and non-biomedical applications.

## Acknowledgments

This work is supported in part by the Engineering Research Center Program of the National Science Foundation under Award Number EEC-0310723 and by a fellowship from the Whitaker Foundation (D.R.). The authors would like to thank Dr. Gerald Loeb and his group members for providing BION chips and testing units. My gratitude also goes to Mr. Trevor Roper and all other members of the Caltech Micromachining Laboratory for assistance with equipment and fabrication.

## References

- [1] W. Li, D.C. Rodger, Y.C. Tai, Integrated wireless neurostimulator, Tech. Digest, in: IEEE International Conference on Micro Electro Mechanical Systems, Sorrento, Italy, January 25–29, 2009.
- [2] Brain and Spinal Cord, available: <http://www.brainandspinalcord.org/brain-injury/statistics.html>.
- [3] The Eye Diseases Prevalence Research Group, Prevalence of age-related macular degeneration in the United States, Arch. Ophthalmol. 122 (2004) 562–572.
- [4] R. Drucker-Colin, L. Verdugo-Diaz, Cell transplantation for Parkinson's disease: present status, Cell. Mol. Neurobiol. 24 (2004) 301–316.
- [5] V. Tropepe, B.L.K. Coles, B.J. Chiasson, D.J. Horsford, A.J. Elia, R.R. McInnes, D.V.D. Kooy, Retinal stem cells in the adult mammalian eye, Science 287 (2000) 2032–2036.
- [6] R.E. Maclaren, R.A. Pearson, A. MacNeil, R.H. Douglas, T.E. Salt, M. Akimoto, A. Swaroop, J.C. Sowden, R.R. Ali, Retinal repair by transplantation of photoreceptor precursors, Nature 444 (2006) 203–207.
- [7] W. Mokwa, Medical implants based on microsystems, Mater. Sci. Technol. 18 (2007) 47–57.
- [8] N.A. Sachs, G.E. Loeb, Development of a BIONic muscle spindle for prosthetic proprioception, IEEE Trans. Biomed. Eng. 54 (1997) 1031–1041.
- [9] J. Kutznerberger, B. Domurath, D.S. Sauerwein, Spastic bladder and spinal cord injury: Seventeen years of experience with sacral deafferentation and implantation of an anterior root stimulator, Artif. Organs 29 (2005) 239–241.
- [10] P. Federspil, P.K. Plinkert, Restoring hearing with active hearing implants, Biomed. Technol. 49 (2004) 76–82.
- [11] W.H. Dobelle, M.G. Mladejovsky, Phosphenes produced by electrical stimulation of human occipital cortex, and their application to the development of a prosthesis for the blind, J. Physiol. 243 (1974) 553–576.
- [12] M. Javaheri, D.S. Hahn, R.R. Lakhnjal, J.D. Weiland, M.S. Humayun, Retinal prostheses for the blind, Ann. Acad. Med. 35 (2006) 137–144.
- [13] T. Stieglitz, W. Haberger, C. Lau, M. Goertz, Development of an inductively coupled epiretinal vision prosthesis, Tech. Digest, in: International IEEE Engineering in Medicine and Biology Society Meetings, San Francisco, CA, USA, September 1–5, 2004.
- [14] J.F. Rizzo, J.L. Wyatt, J. Loewenstein, S. Montezuma, D.B. Shire, L. Theogarajan, S.K. Kelly, Development of a wireless, ab externo retinal prosthesis, Invest. Ophthalmol. Vis. Sci. 45 (2004) 3399.
- [15] W. Li, D.C. Rodger, E. Meng, J.D. Weiland, M.S. Humayun, Y.C. Tai, Flexible parylene packaged intraocular coil for retinal prostheses, Tech. Digest, in: International IEEE-EMBS Special Topic Conference on Microtechnologies in Medicine and Biology, Okinawa, Japan, May 9–12, 2006.
- [16] D.C. Rodger, A.J. Fong, W. Li, H. Ameri, A.K. Ahuja, C. Gutierrez, I. Lavrov, H. Zhong, P. Menon, E. Meng, J.W. Burdick, R.R. Roy, V.R. Edgerton, J.D. Weiland, M.S. Humayun, Y.C. Tai, Flexible parylene-based multielectrode arrays technology for high-density neural stimulation and recording, Sens. Actuators B: Chem. 132 (2008) 449–460.
- [17] L. Wolgemuth, Assessing the performance and suitability of parylene coating, Med. Device Diagn. Ind. 22 (2000) 42–49.
- [18] D.C. Rodger, J.D. Weiland, M.S. Humayun, Y.C. Tai, Scalable flexible chip-level parylene package for high lead count retinal prostheses, Tech. Digest, in: International Conference on Solid-State Sensors, Actuators, and Microsystems, Seoul, Korea, June 5–9, 2005.
- [19] H.B. Dwight, Electrical Coils and Conductors, McGraw-Hill, New York, 1945 (Chapter 31, p. 267).
- [20] P.J. Chen, W.C. Kuo, W. Li, Y.J. Yang, Y.C. Tai, Q-enhanced fold-and-bond MEMS inductors, Tech. Digest, in: IEEE International Conference on Nano/Micro Engineering and Molecular Systems, Sanya, Hainan, China, January 6–9, 2008.
- [21] T. Harder, T.J. Yao, Q. He, C.Y. Shih, Y.C. Tai, Residual stress in thin-film parylene C, Tech. Digest, in: IEEE International Conference on Micro Electro Mechanical Systems, Las Vegas, NV, USA, January 20–24, 2002.
- [22] W. Li, D.C. Rodger, Y.C. Tai, Implantable RF-coiled chip packaging, Tech. Digest, in: IEEE International Conference on Micro Electro Mechanical Systems, Tucson, AZ, USA, January 13–17, 2008.
- [23] U.K. Mudali, T.M. Sridhar, B. Raj, Corrosion of bio implants, Sadhana 28 (2003) 601–637.
- [24] W. Li, D.C. Rodger, P. Menon, Y.C. Tai, Accelerated-lifetime soak testing of parylene packaging, Tech. Digest, in: ACS 235th National Meeting, New Orleans, LA, USA, April 6–10, 2008.
- [25] A.C. Dupont, S.D. Bagg, J.L. Creasy, C. Romano, D. Romano, F.J.R. Richmond, G.E. Loeb, First clinical experience with BION implants for therapeutic electrical stimulation, Neuromodulation 7 (2004) 38–47.
- [26] M.A. Fonseca, M.G. Allen, J. Kroh, J. White, Flexible wireless passive pressure sensors for biomedical applications, Tech. Digest, in: 12th Solid-State Sensors



and Actuators, Microsystems Workshop, Hilton Head Island, SC, USA, June 4–8, 2006.

## Biographies

**Wen Li** received her PhD in 2008 and MS in 2004 in electrical engineering from California Institute of Technology. Prior to that, she studied at Tsinghua University and received an MS degree in microelectronics in 2003 and a BS degree in material science and engineering in 2001. Dr. Li is currently an assistant professor of electrical and computer engineering at the Michigan State University. Her research interests include MEMS/NEMS technologies and systems, micro sensors and actuators, biomimetic devices and systems, microfluidic and lab-on-chip systems, and microsystem integration and packaging technologies. She is a member of the Institute of Electrical and Electronics Engineers, the Eta Kappa Nu, and the American Chemical Society.

**Damien C. Rodger** received his BS in electrical engineering (magna cum laude with honors) from Cornell University in 2000, and his PhD in bioengineering from the California Institute of Technology in 2008. He earned his MD at the Keck School of Medicine of the University of Southern California in 2009 and conducts research on microtechnologies for retinal and spinal cord prostheses and on other novel bioMEMS for ophthalmic use. He will be pursuing a residency in ophthalmology at the Doheny Eye Institute in Los Angeles, CA. He held a Whitaker Foundation Graduate Fellowship from 2003 to 2006 and is a member of the IEEE EMBS and the Association for Research in Vision and Ophthalmology (ARVO).

**Anderson Pinto** received his MD from University Severino Sombra, Rio de Janeiro, Brazil. He completed his residency in Ophthalmology at University of Mogi das Cruzes, São Paulo, Brazil. After that, he went to Federal University of São Paulo, Brazil, for a Fellowship in retina and vitreous. He also earned a PhD degree from the same university. Currently, he is a post-doctoral student at the Doheny Eye Institute in Los Angeles, CA.

**Ellis Meng** received the BS degree in engineering and applied science and the MS and PhD degrees in electrical engineering from the California Institute of Technology (Caltech), Pasadena, in 1997, 1998, and 2003, respectively. Since 2004, she has been an Assistant Professor in the Department of Biomedical Engineering, University of Southern California, Los Angeles. She holds a joint appointment in the Ming Hsieh Department of Electrical Engineering. Her research interests include bioMEMS, implantable biomedical microdevices, microfluidics, multimodality inte-

grated microsystems, and packaging. Currently, she is the Thrust Leader for Interface Technology in the National Science Foundation Biomimetic MicroElectronic Systems Engineering Research Center (BMES ERC). She also holds the Viterbi Early Career Chair in the Viterbi School of Engineering. Dr. Meng is a member of Tau Beta Pi, Biomedical Engineering Society, Society of Women Engineers, and American Society for Engineering Education. She was a recipient of the Intel Women in Science and Engineering Scholarship, Caltech Alumni Association Donald S. Clark Award, and Caltech Special Institute Fellowship. She has also received the NSF CAREER and Wallace H. Coulter Foundation Early Career Translational Research awards.

**James D. Weiland** received his BS from the University of Michigan in 1988. After 4 years in industry with Pratt & Whitney Aircraft Engines, he returned to Michigan for graduate school, earning degrees in biomedical engineering (MS in 1993, PhD in 1997) and electrical engineering (MS in 1995). In 1999 he was appointed an assistant professor of ophthalmology at Johns Hopkins. Dr. Weiland is now the Director of the Intraocular Retinal Prosthesis Lab at the Doheny Retina Institute, and is an associate professor of ophthalmology and biomedical engineering at the University of Southern California. He is a member of the IEEE EMBS, the Biomedical Engineering Society, and the Association for Research in Vision and Ophthalmology.

**Mark S. Humayun** received his BS from Georgetown University in 1984, his MD from Duke University in 1989, and his PhD from the University of North Carolina, Chapel Hill in 1994. He finished his training by completing an Ophthalmology residency at Duke and a Fellowship in Vitreoretinal Diseases at Johns Hopkins Hospital. Currently, Dr. Humayun is a professor of ophthalmology, biomedical engineering, and cell and neurobiology at the University of Southern California. Dr. Humayun is the Director of the National Science Foundation Biomimetic MicroElectronic Systems Engineering Research Center (BMES ERC) and the Director for the Department of Energy Artificial Retina Project that is a consortium of five Department of Energy labs and four universities, as well as industry. He is also a member of the National Academies Institute of Medicine and the Institute of Electrical and Electronics Engineers (IEEE).

**Yu-Chong Tai** is a Professor of Electrical Engineering, Mechanical Engineering and Bioengineering at the California Institute of Technology. He developed the first electrically spun polysilicon micromotor at UC Berkeley. At Caltech, his main research interest is MEMS for biomedical applications including lab-on-a-chip and neural implants. He has published more than 300 technical articles in the field of MEMS. He is the recipient of the IBM Fellowship, Ross Tucker Award, Best Thesis Award (at Berkeley), Presidential Young Investigator (PYI) Award, Packard Award and ALA Achievement Award. He is a fellow of IEEE.